

ANL/CMT/CP-87764
CONF-9510241--1

RECEIVED

NOV 21 1995

OSTI

DEVELOPING A DYNAMIC MODEL OF A METHANOL STEAM REFORMER
FOR USE IN A FUEL CELL PROPULSION SYSTEM*

H. K. Geyer, R. K. Ahluwalia, R. Kumar, and M. Krumpelt

DISCLAIMER

This report was prepared as an account of work sponsored by an agency of the United States Government. Neither the United States Government nor any agency thereof, nor any of their employees, makes any warranty, express or implied, or assumes any legal liability or responsibility for the accuracy, completeness, or usefulness of any information, apparatus, product, or process disclosed, or represents that its use would not infringe privately owned rights. Reference herein to any specific commercial product, process, or service by trade name, trademark, manufacturer, or otherwise does not necessarily constitute or imply its endorsement, recommendation, or favoring by the United States Government or any agency thereof. The views and opinions of authors expressed herein do not necessarily state or reflect those of the United States Government or any agency thereof.

Argonne National Laboratory
9700 South Cass Avenue
Argonne, Illinois 60439

EXTENDED ABSTRACT
of paper to be presented at
U. S. Department of Energy's
Automotive Technology Development
Contractors' Coordination Meeting
ATD-CCM 1995

October 23-27, 1995
Dearborn, MI

The submitted manuscript has been authored by a contractor of the U. S. Government under contract No. W-31-109-ENG-38. Accordingly, the U. S. Government retains a nonexclusive, royalty-free license to publish or reproduce the published form of this contribution, or allow others to do so, for U. S. Government purposes.

*This research was supported by the U. S. Department of Energy, Electric and Hybrid Propulsion Systems Division, Office of Transportation Technologies, under contract number W-31-109-Eng-38.

MASTER

DISTRIBUTION OF THIS DOCUMENT IS UNLIMITED

at

DEVELOPING A DYNAMIC MODEL OF A METHANOL STEAM REFORMER FOR USE IN A FUEL CELL PROPULSION SYSTEM

H. K. Geyer, R. K. Ahluwalia, R. Kumar, and M. Krumpelt
Argonne National Laboratory
Argonne, Illinois 60439

Introduction

Transportation fuel cell systems are being developed for methanol as the on-board fuel instead of the difficult-to-store hydrogen. Two such systems under development include polymer electrolyte and phosphoric acid fuel cells (PEFC, PAFC), which operate at 80°C and 200°C, respectively. Because of these relatively low operating temperatures, the methanol must be converted to a hydrogen-rich gas before it can be fed to the fuel cell stack (except in the case of the direct electrochemical oxidation of methanol, presently under development). Steam reforming of methanol is used in the PAFC buses developed by H-Power Corp. [1]. A methanol steam reformer is also being developed by General Motors (GM) for light-duty vehicle PEFC systems [2]. Earlier, we described results from steady-state and off-design simulations of methanol-fueled PEFC systems [3]. These results indicated that the dynamic response of the fuel cell system is likely governed by the transient performance of the methanol reformer (rather than the dynamic performance of the fuel cell stack or other balance-of-plant components). This paper discusses the development of a dynamic model for the methanol steam reformer, which will subsequently be used in simulating the dynamic performance of the complete fuel cell system.

The Reformer Model

The model assumes cylindrical tubes packed with the reforming catalyst heated by hot combustion gases generated by burning the spent anode gas and/or fresh methanol. The hot gas flows in an annulus surrounding the catalyst tube (Fig. 1). The model can also handle recirculating reformate gas flows. Both the process and combustion gases are treated as ideal gases and ideal gas mixtures. Modeling of the gas flows assumes constant pressures and flows only in the $\pm z$ direction (co-flow as well as counter-flow) and includes equations for species conservation, convective diffusion, and conservation of energy. Assumptions made for the species conservation equation include frozen chemistry for the combustion hot gas, and a single-species diffusion coefficient for the convective diffusion equation. The species conservation equation is used to calculate the methanol concentration in the process gas stream. Optionally, it is also used to calculate the water concentration, depending on whether or not the water-gas shift reaction is included in the calculations; this option is used to study the significance of the water-gas shift reaction on methanol conversion rates and the hydrogen concentration in the product gas. The conservation of energy formulation

uses either separate temperatures for the catalyst particles and the process gas or a single temperature for the two. The single-temperature case is a simplification of the more rigorous two-temperature case and produces a reasonably accurate solution with less computational time. The two-temperature case includes heat transfer within the process gas, heat transfer between the catalyst pellets and the process gas, and the heats of reactions.

The model will determine the temperature profiles of the process gas and the catalyst particles within the catalyst tube, the tube walls, and the hot gas flowing in the annulus. The reaction kinetics used in the model are based on published reaction rates [4-8]. The model has been used for three types of simulations: operation at constant temperatures, steady-state operation, and start-up and transient operation.

Methanol Conversions at Constant Temperatures

The accuracy of the reaction rates used in the model can be assessed by comparing the calculated methanol conversion with the experimentally measured values. This can be done by using the constant temperature option. With this option, only the residence time (reactor length) is relevant, defined as the amount of catalyst (in kg) divided by the inlet flow rate of the methanol (kg/s or mol/s), or W/F . Note that while the reduced units of W/F may be seconds, this is not the gas residence time, since the gas and the catalyst have different densities. The other significant variable is the molar ratio of water to methanol (denoted as b). Typically b is in the range of 1.3 to 1.5; however, the published reaction rates also include data at $b=0.67$, and this value was also used in some of our reformer simulations. Figure 2 shows the calculated and measured methanol conversion versus temperature with a copper-zinc oxide catalyst. The calculated values were obtained for $W/F=500$ kg-s/mol and $b=1.5$. The experimental data lie within the curve assuming shift equilibrium and the curve based on the shift kinetics. Figure 3 shows that the methanol conversion with the copper-zinc oxide catalyst is affected most strongly by the reaction temperature, and much less strongly by the relative amount of catalyst (W/F). The methanol conversion was 99% or better at temperatures $\geq 250^\circ\text{C}$ and $b=1.0$.

Steady-State Operation

In an actual steam reformer, the heat of reaction is provided by the hot combustion gases, so that the catalyst temperature is not constant but varies in the radial and axial directions. Since the reaction kinetics are a strong function of temperature, these temperature variations can have a pronounced effect on methanol conversion. The effects of various length-to-diameter ratios and the ratios of hot-gas to process-gas flow rates (m_g/m_r) were examined. For the results given here, the pressures were set to 1 atm, the inlet methanol/water temperature to 400 K (i.e., vaporized), and the inlet hot gas temperature to 900 K. The reactor length was set to 1 m. Although the reformer is essentially a heat exchanger, the reaction energies greatly affect the temperature distribution compared to that obtained for a simple heat exchanger. This difference is illustrated in Fig. 4 using the single-temperature option discussed above. Without the endothermic reaction, there is no heat exchange beyond about 0.5 m; with the reaction, some heat transfer is still occurring at the tube exit. Thus, to obtain high methanol conversions, it would not be effective to design the reformer purely on heat exchange principles. Figure 5 shows that for $m_g/m_r=2.0$ and 3.2, the process gas temperature increases rapidly within the first 5 to 10 cm and then changes more gradually along the length of the reformer tube. The conversion of methanol (Fig. 6) is strongly affected by the gas flow

rates, approaching 100% for high values of m_g/m_r , but only 80% for lower values of m_g/m_r . Figure 7 shows the effect of catalyst tube diameter on the temperature profiles. The larger tubes have a lower temperature at the center near the process gas inlet, leading to slightly lower methanol conversion rates, i.e., 96.85% conversion in 5-cm dia tubes compared to 99.96% conversion in 1-cm dia tubes.

Start-up and Transient Simulations

To simulate a cold start-up, the combustion gas velocity was increased to its steady-state design value and its temperature to 900 K in 1 s. The inlet fuel flow rate was increased to its design value and its temperature raised to 400 K in 60 s (to avoid condensation in the catalyst bed). Figure 8 shows the methanol conversion rates as a function of time for 1-cm and 5-cm dia reformer tubes. For the larger tube, over 900 s was required to reach 50% conversion, and even at 1500 s, only 81% of the feed methanol was converted. Conversion in the thinner tube reached 50% in 520 s and 96% in 1500 s. The peak bed temperature and the process gas exit temperature are shown in Fig. 9 for the two tube diameters. Figure 10 shows the hydrogen concentration in the process gas leaving the reformer as a function of time. Profiles of temperature and methanol conversion for the 1-cm dia tubes are shown in Figs. 11 and 12. These figures clearly show how the thermal energy input gradually heats up the reformer from the inlet to the exit, and that the bulk of the methanol conversion occurs in the first one-third of the catalyst bed.

For a recirculating gas reformer, shown schematically in Fig. 13, the effects of varying the recycle ratio on methanol conversion and the exit temperature of the process gas at steady state are shown in Figs. 14 and 15. Increasing the recycle ratio beyond 4 has little effect on the conversion of methanol. However, the exit temperature continues to increase as the recycle ratio is increased to about 12.

Acknowledgment

This research was supported by the U. S. Department of Energy, Electric and Hybrid Propulsion Systems Division, Office of Transportation Technologies, under contract number W-31-109-Eng-38.

References

1. "Phosphoric Acid Fuel Cell Bus Development," A. Kaufman, Proceedings of the Annual Automotive Technology Development Contractors' Coordination Meeting 1994, Society of Automotive Engineers, Inc., Warrendale, PA, P-289, ISBN 1-56091-654-0, April 1995, pp. 289-293.
2. "PEM Fuel Cell System R&D for Light-Duty Vehicles—Technical Scope," M. H. Fronk, G. W. Skala, N. E. Vanderborgh, and K. R. Stroh, Proceedings of the Annual Automotive Technology Development Contractors' Coordination Meeting 1994, Society of Automotive Engineers, Inc., Warrendale, PA, P-289, ISBN 1-56091-654-0, April 1995, pp. 283-287.
3. "Modeling of Polymer Electrolyte Fuel Cell Systems," R. Kumar, R. Ahluwalia, H. K. Geyer, and M. Krumpelt, Proceedings of the Annual Automotive Technology Development Contractors' Coordination Meeting 1993, Society of Automotive Engineers, Inc., Warrendale, PA, P-278, ISBN 1-56091-539-0, May 1994, pp. 409-417.

4. "Hydrogen Production by the Catalytic Steam Reforming of Methanol. Part 1: The Thermodynamics," J. C. Amphlett, M. J. Evans, R. A. Jones, R. F. Mann, and R. D. Weir, *Can. J. Chem. Eng.*, Vol 59, December 1981.
5. "Hydrogen Production by the Catalytic Steam Reforming of Methanol. Part 1: Kinetics of Methanol Decomposition Using Girdler G66B Catalyst," J. C. Amphlett, M. J. Evans, R. F. Mann, and R. D. Weir, *Can. J. Chem. Eng.*, Vol 63, August 1985.
6. "Hydrogen Production by the Catalytic Steam Reforming of Methanol. Part 1: Kinetics of Methanol Decomposition Using C18HC Catalyst," J. C. Amphlett, R. F. Mann, and R. D. Weir, *Can. J. Chem. Eng.*, Vol 66, December 1988.
7. "Production of Hydrogen-Rich Gas by Steam Reforming of Methanol over Copper Oxide-Zinc Oxide Catalysts," J. C. Amphlett, R. F. Mann, C. McKnight, and R. D. Weir, *Proc. 20th IECEC*, Miami Beach, FL, August 1985.
8. "Kinetic Study of Steam Reforming of Methanol over Copper-Based Catalysts," C. J. Jiang, D. L. Trimm, and M. S. Wainwright, *Appl. Catalysis A: General*, 93, 1993.

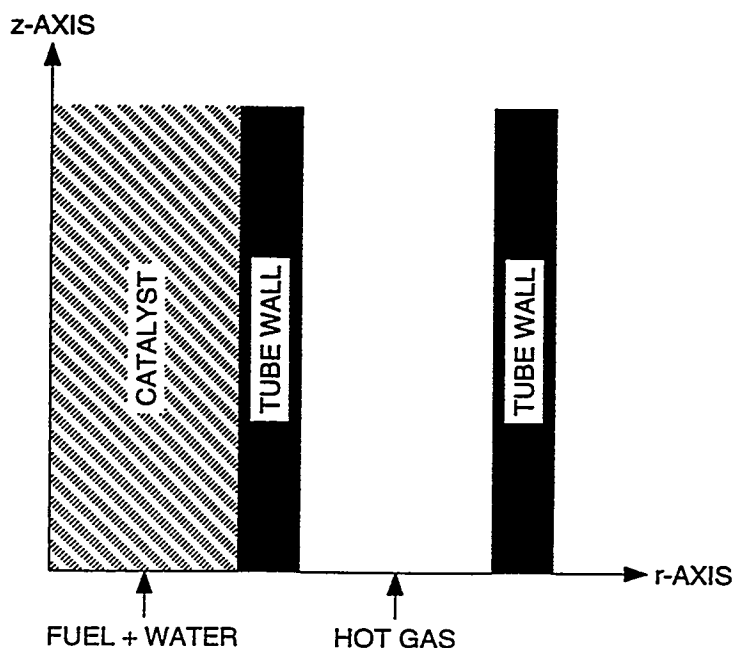


Fig. 1. Typical reformer geometry.

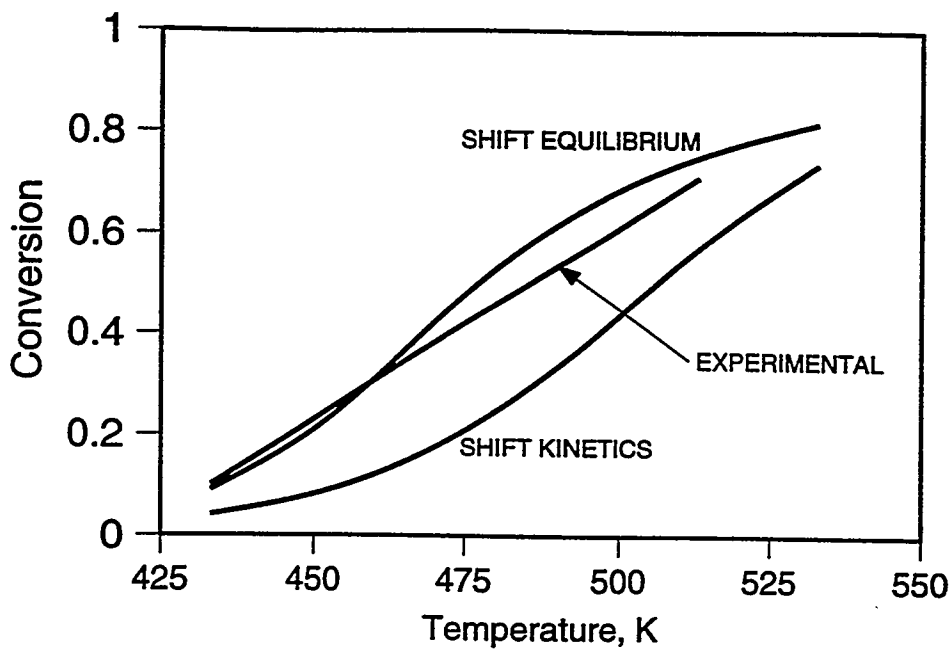


Fig. 2. Methanol conversion with the copper-zinc oxide catalyst (G66B) as a function of temperature. $W/F=500$ kg-s/mol; $b=1.5$.

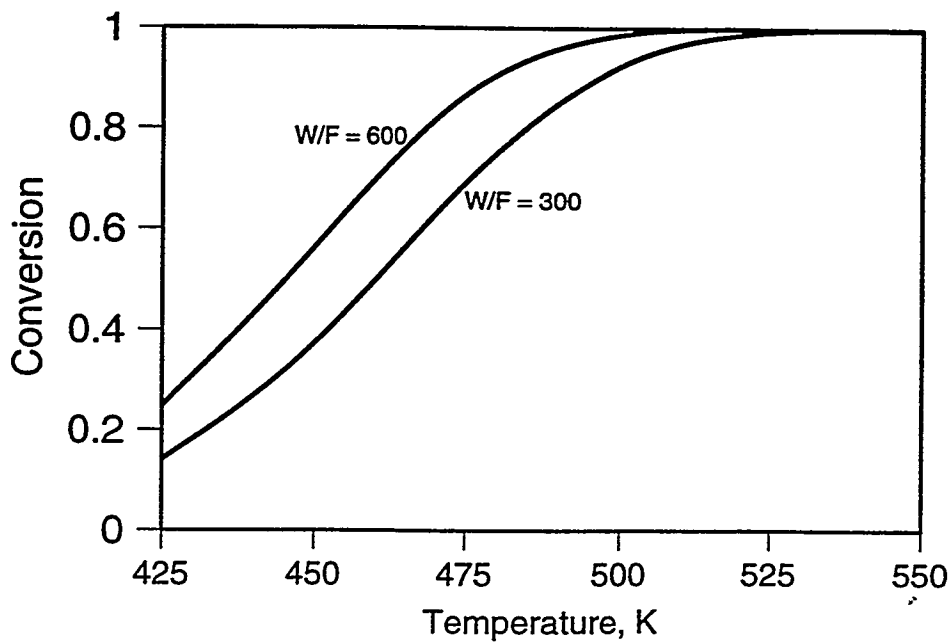


Fig. 3. Methanol conversion with copper-zinc oxide catalyst (C18HC) as a function of temperature and catalyst-to-feed ratio for $b=1.0$.

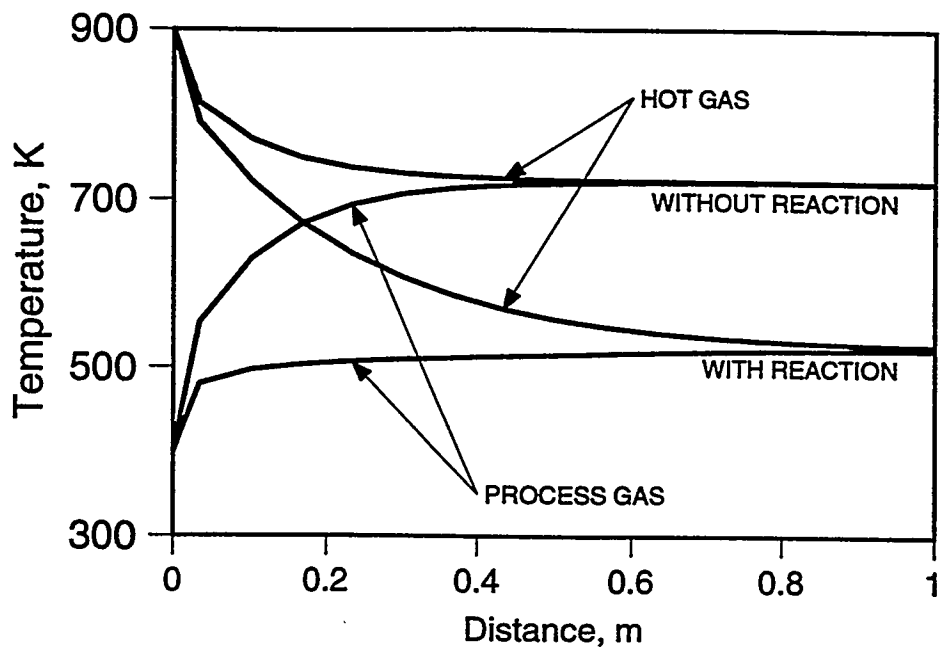


Fig. 4. Axial temperature distributions with and without the steam reforming reactions.

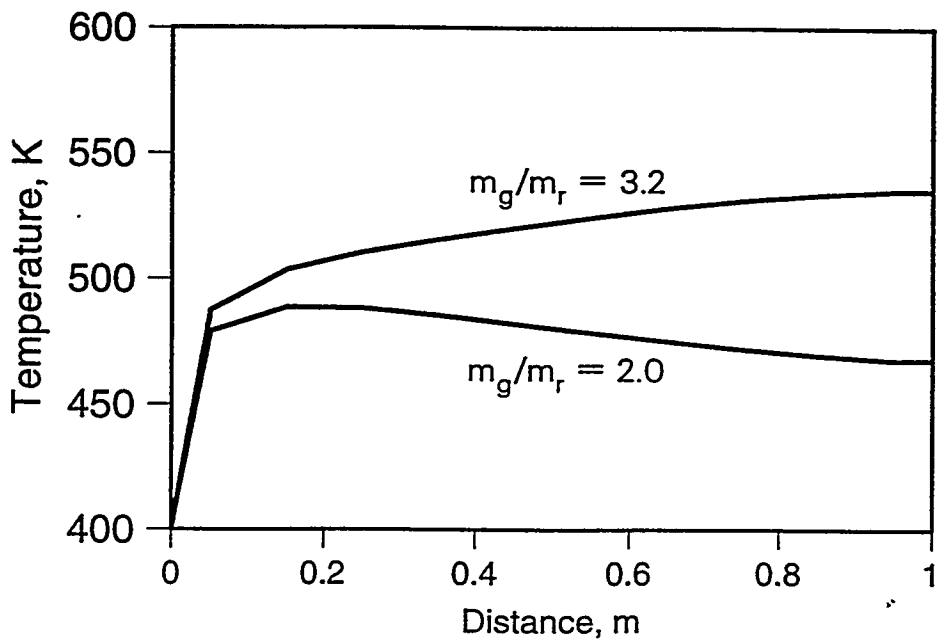


Fig. 5. Axial temperature distributions for $W/F = 400$ kg-s/mol and m_g/m_r ratios of 2.0 and 3.2.

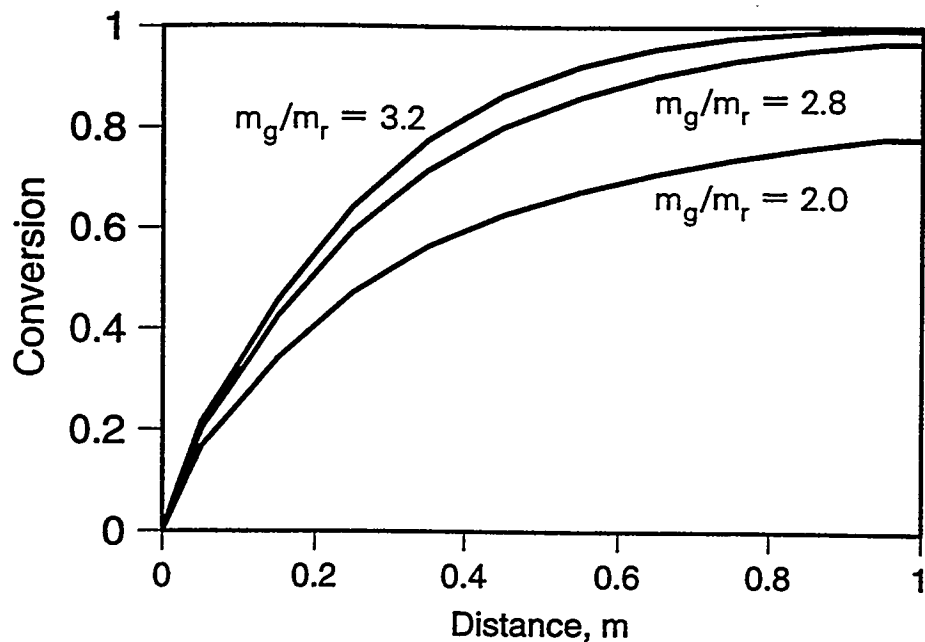


Fig. 6. Methanol conversion along the length of the C18HC catalyst bed for $W/F = 400 \text{ kg-s/mol}$ and different m_g/m_r ratios.

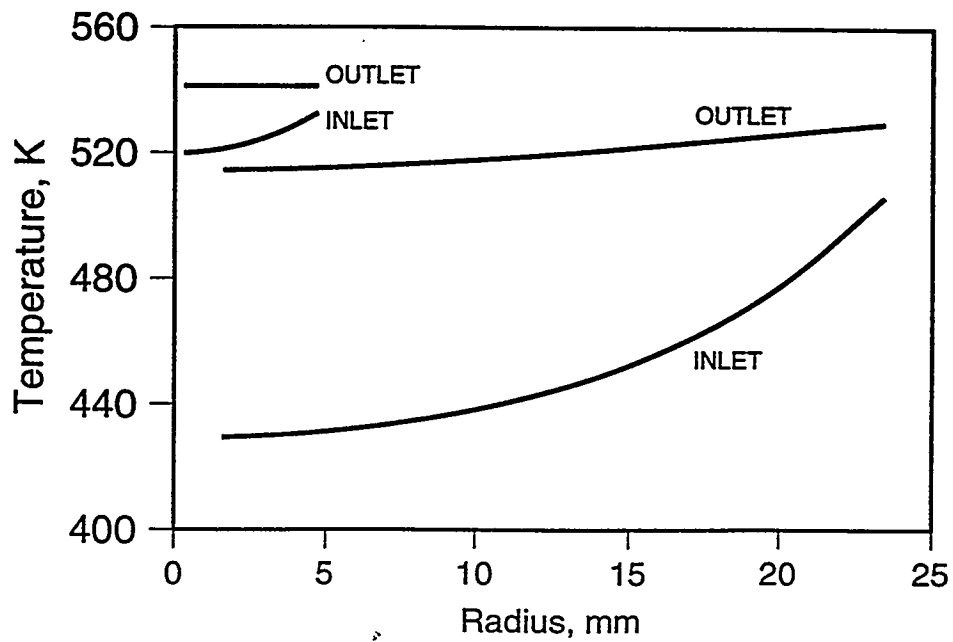


Fig. 7. Radial temperature distributions near the inlet and exit from catalyst tubes of 1-cm and 5-cm dia (5-mm and 25-mm radius).

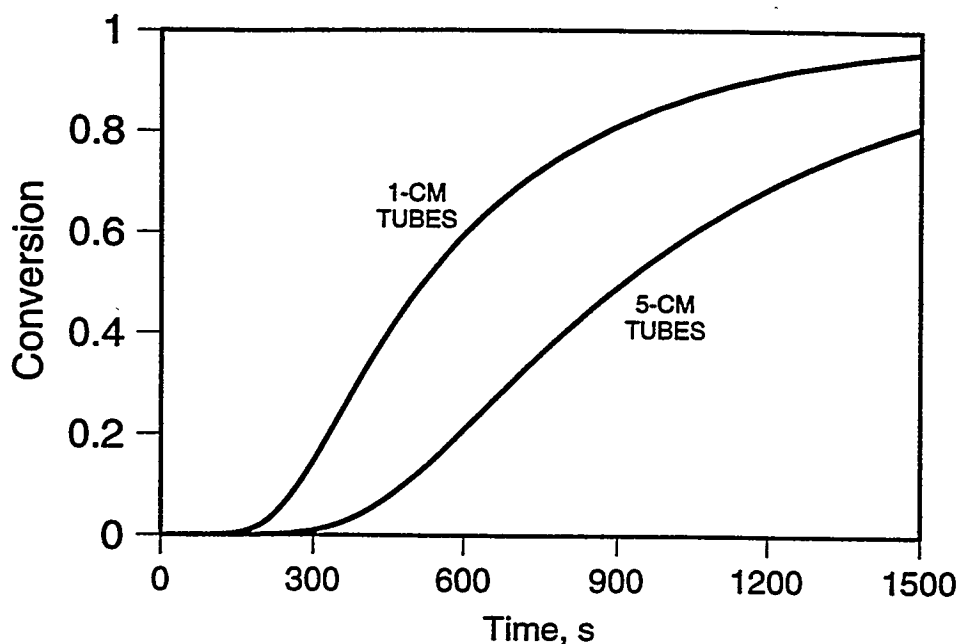


Fig. 8. Methanol conversion as a function of time during start-up of the steam reformer with 1-cm and 5-cm dia catalyst tubes.

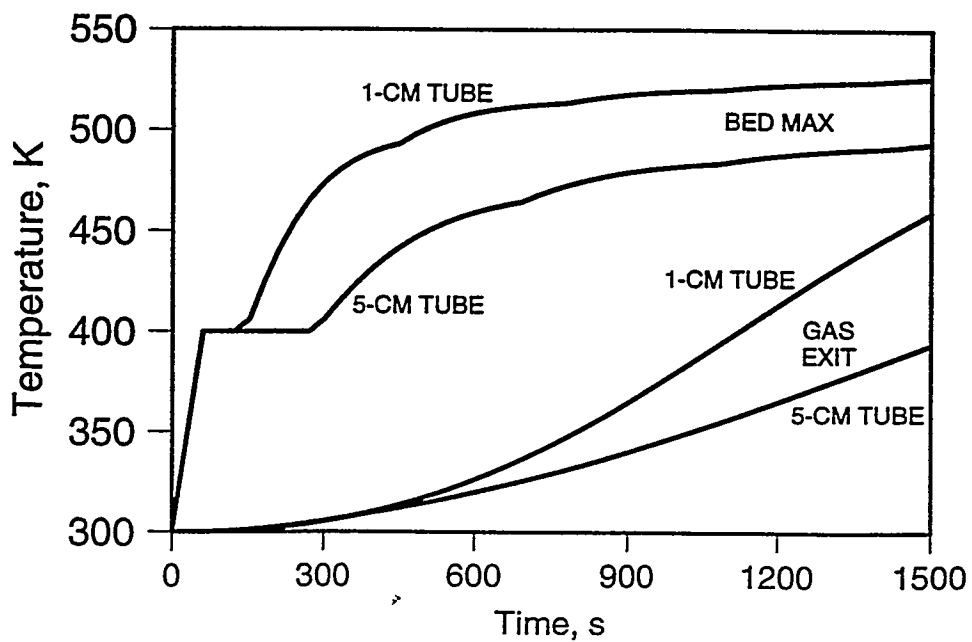


Fig. 9. Peak catalyst temperatures and the process gas exit temperatures during start-up of the steam reformer with 1-cm and 5-cm dia catalyst tubes.

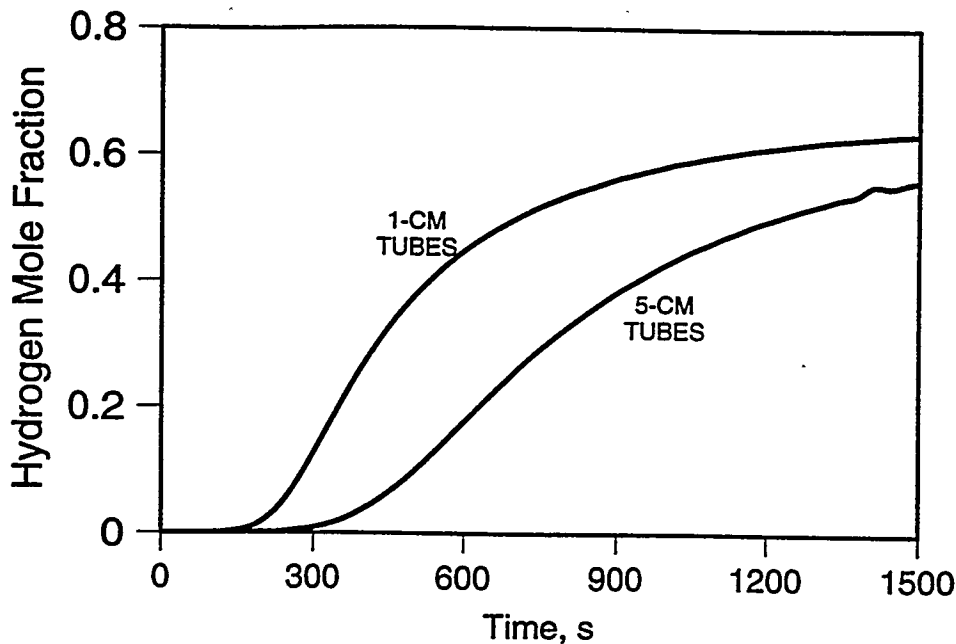


Fig. 10. Hydrogen concentration in the process gas leaving the reformer during start-up for 1-cm and 5-cm dia catalyst tubes.

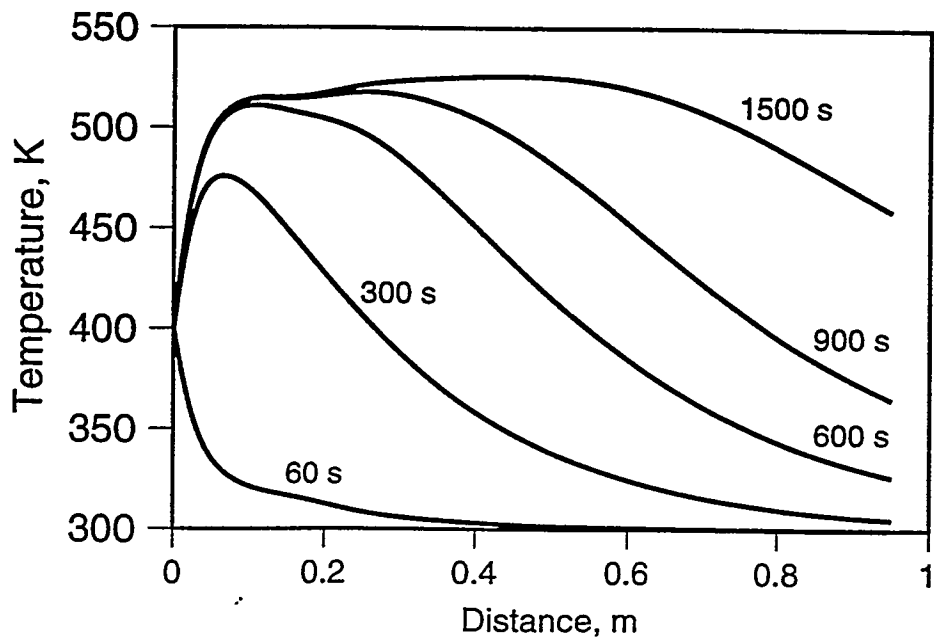


Fig. 11. Axial temperature profiles in the 1-cm dia catalyst tubes during reformer start-up for the first 1500 s.

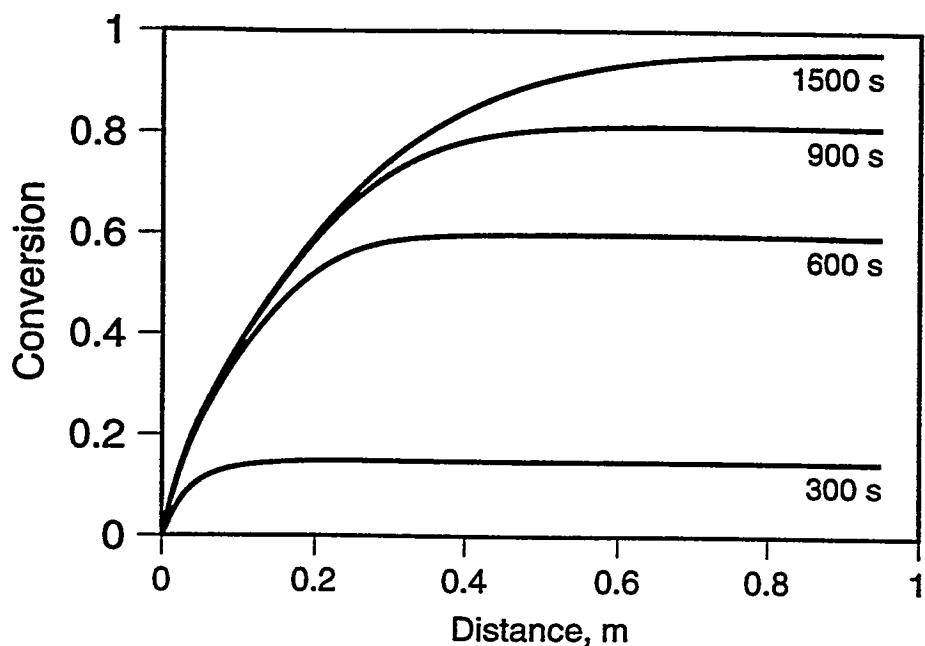


Fig. 12. Axial profiles of methanol conversion in the 1-cm dia catalyst tubes during reformer start-up for the first 1500 s.

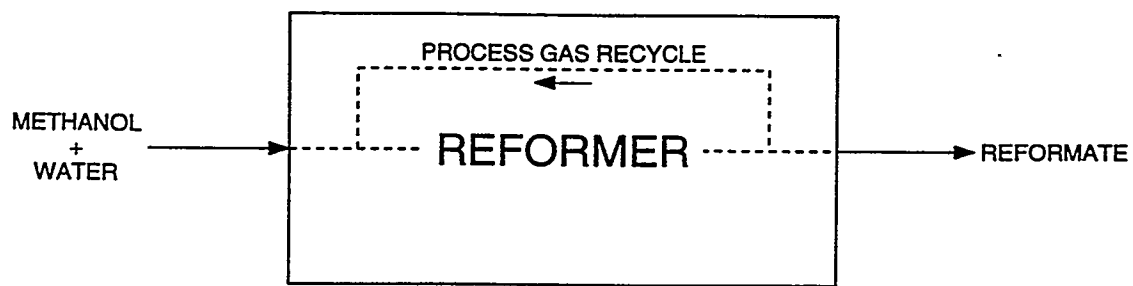


Fig. 13. Schematic diagram of the steam reformer with recirculating process gas.

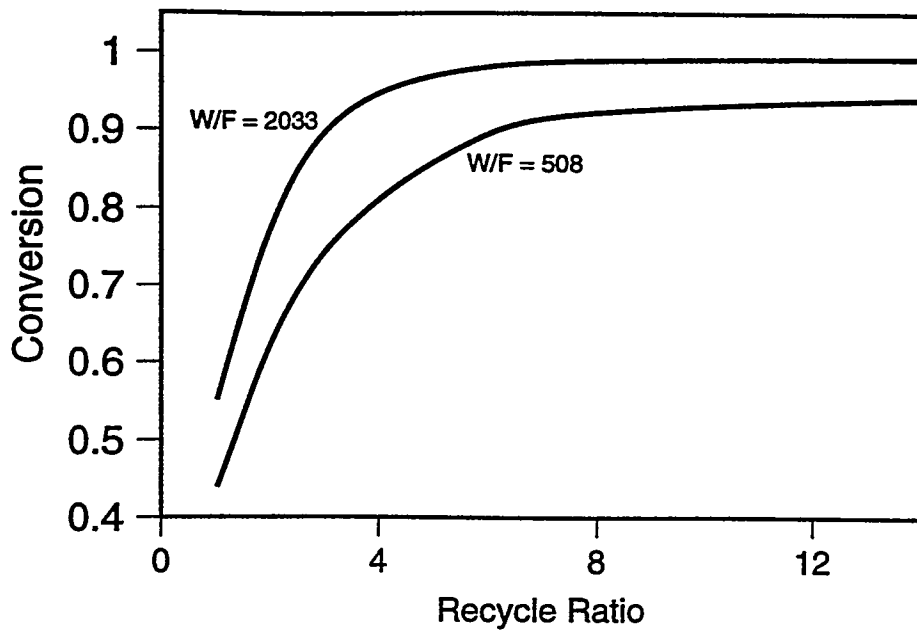


Fig. 14. Methanol conversion versus recycle ratio for reformer of Fig. 13.

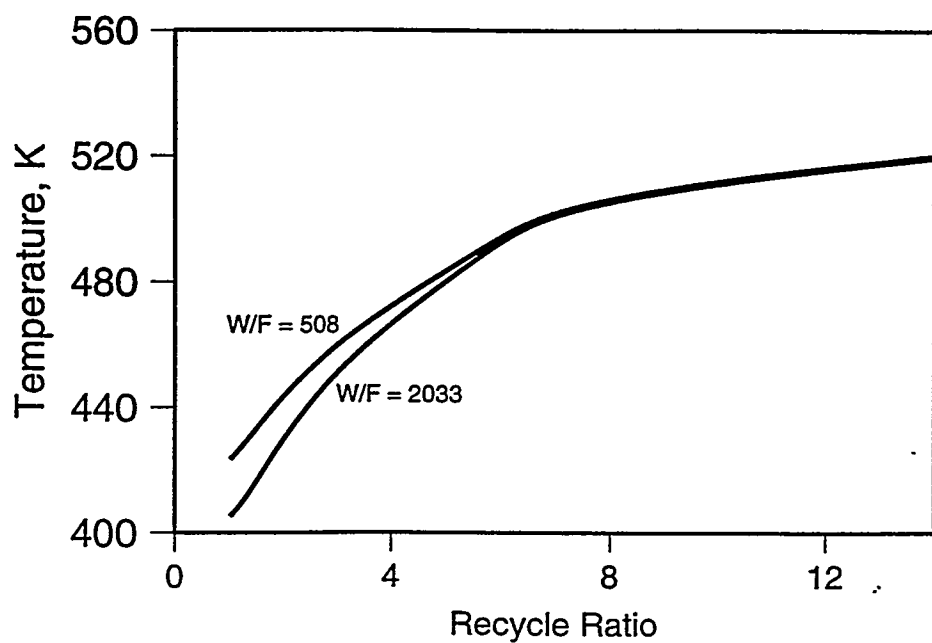


Fig. 15. Exit temperature versus recycle ratio for reformer of Fig. 13.